Mineralogical Magazine doi: 10.1180/mgm.2020.7

Geochemical fingerprints of brannerite (UTi_2O_6): an integrated study

Marion Turuani, Flavien Choulet*, Aurélien Eglinger, Philippe Goncalves, Julie Machault, Julien Mercadier, Anne-Magali Seydoux-Guillaume, Stephanie Reynaud, Fabien Baron, Daniel Beaufort, Yann Batonneau, Sophie Gouy, Adel Mesbah, Stéphanie Szenknect, Nicolas Dacheux, Virginie Chapon, Maurice Pagel

***Author for correspondence:** Flavien Choulet, Email: flavien.choulet@univ-fcomte.fr

Appendix

Geological setting of studied brannerite samples

Geological setting of hydrothermal brannerite

La Gardette Mine (GD) is located in Western French Alps close to Bourg-d'Oisans city. Alpine-type quartz veins crosscut the amphibolite of the Variscan basement and its Triassic carbonate cover (Barféty *et al.*, 1972). Ore minerals include native gold, galena, pyrite, chalcopyrite, tennantite and brannerite (Geffroy, 1963). Age of mineralisation is currently unknown but it could be related to Upper Miocene (ca. 5–11 Ma) episodes of hydrothermal fluid circulation recorded in the Belledonne Massif to the Northwest (Gasquet *et al.*, 2010).

The Bou Azzer (BA) deposit is located in the Moroccan Anti Atlas Belt. It occurs within a Proterozoic ophiolitic unit covered by unconformable Palaeozoic sedimentary rocks (Leblanc and Billaud, 1982). Bou Azzer is classified as a particular case of Five-Element Vein-Type deposits (Leblanc, 1986; Kissin, 1992); it is currently mined for Co Ni, Ag and Au. The polyphase mineralisation includes an early Ni-Co-Fe arsenide stage followed by a late Cu-Zn-Fe sulfide stage (Ennaciri *et al.*, 1997) related to high salinity brines (Leblanc and Lbouabi, 1988). While uraninite is present throughout the whole mineralisation evolution, brannerite only occurs during the latest stage in association with molybdenite, chlorite, and quartz (Ennaciri, 1995). Brannerite stage has been dated by U-Pb LA-ICPMS method at 310 ± 5 Ma (Oberthür *et al.*, 2009).

Brannerite (HL) was collected in the Chhuling Khola Valley in Nepal. This area consists of a series of schists, gneisses, and migmatites that belong to the Greater Himalayan Sequence, which is thrusted over the low-grade metamorphic rocks of the Lesser Himalayan Sequence, along the Main Central Thrust (Pêcher, 1989). Among these high-grade gneisses, an albitised and U-mineralised zone is exposed (Maruejol, 1988). While biotite gneisses have recorded an early sodic metasomatic stage coeval with ductile deformation along the MCT, brannerite co-precipitated with secondary albite in brittle veins forming a stockwork zone. Formation of brannerite is considered as the result of alteration of Ti oxides of the biotite gneisses by Na-U alkaline and oxidising fluids (Maruejol, 1988) under low-grade metamorphic conditions. Isotope Dilution termal ionisation mass spectrometry (ID-TIMS) U-Pb dating on brannerite has given a crystallisation $^{206}Pb/^{238}U$ age at 4.8 Ma (Copeland *et al.*, 1991).

The Mont Chemin (MC) mines are located in the eponymous mountain in Western Valais, Switzerland. The mines have been exploited from Middle Age until to the 20th century for Au, Ag, Pb, Fe, and fluorite (Ansermet, 2001). The veins crosscut the metamorphic Variscan basement (external crystalline massif) and particularly small late Palaeozoic granite intrusions within gneisses. At the Tête des Econduits, quartz veins include scheelite, anatase, fluorite, native Au, and brannerite (Meisser, 1998). These Alpine-type veins are probably related to a regional Miocene episode of hydrothermal fluid circulation at *ca* 10 Ma (Marshall *et al.*, 1998).

The Kratka Valley (KV) occurrences are located to the north of Gemerska Poloma between Dobsina and Kosice in Eastern Slovakia. U-bearing quartz veins occur within the Ordovician Vlachovo Formation of the Southern Gemericum Unit (Vozárová *et al.*, 2010). This volcano-sedimentary sequence was further intruded by Permian granites, covered by Mesozoic sediments and affected by Cretaceous regional metamorphism (Vozárová *et al.*, 2014). A wide range of U mineralisation is found within the Gemericum Unit, including U-Mo mineralised horizons, stratiform Cu-U redbeds and U-Mo stockworks (Rojkovic *et al.*, 1993). U–Ti oxides, including brannerite, were reported from several localities (Rojkovic and Boronikhin, 1982). At Kratka Valley, brannerite-bearing quartz veins also contain gold, arsenopyrite, chalcopyrite, molybdenite, pyrite, rutile, uraninite as well as many secondary U minerals. Timing of brannerite formation is currently unknown, but Lower Jurassic (Števko *et al.*, 2014) and Lower Cretaceous (Rojkovic *et al.*, 1993) mineralizing events have been reported in the area.

Geological setting of pegmatitic brannerite

The Crocker's Well (CW) prospect, located in the southern part of Central Australia is a uranium occurrence discovered in 1951. Ore is hosted by peraluminous sodic granitoids, mainly adamellite and trondhjemite, and minor sodic gneisses (Ashley, 1984, and reference therein). Emplacement of this suite has been dated by zircon ID-TIMS (isotopic Dilution Thermal ionisation Mass spectrometry) U-Pb at 1579.2 ± 1.5 Ma (Ludwig and Cooper, 1984). Although the distribution of brannerite is controlled by fractures (Campana and King, 1958), the vein systems and the mineralised breccia are restricted to the host granite, which did not experience hydrothermal alteration. Brannerite is associated with quartz, F-bearing phlogopite, sodic plagioclase, fluorapatite, niobian rutile, monazite, muscovite, chlorite, tourmaline, and fluorite (Ashley, 1984). Brannerite formation probably results from the evolution of a late peraluminous magmatic system, as indicated by the younger $^{206}Pb/^{238}U$ ages obtained directly on brannerite (550–572 Ma, Ludwig and Cooper, 1984). In this sense, Crocker's Well uranium occurrence shares many analogies with Rössing and Limousin types (e.g. Cuney, 2010), with the exception of the sodic enrichment.

The Hidden Valley (HV) area is located at Brannerite Hill in the North Finders Ridge in south Central Australia. This area is characterised by Mesoproterozoic migmatitic gneisses associated with Neoproterozoic metasediments and volcanics (Coats and Blissett, 1971), which recorded metamorphism related to the

Delamerian orogeny (Foden *et al.*, 2006). Palaeozoic leucogranites and pegmatites dated around 450 Ma are intrusive within this metamorphic sequence (Wülser, 2009). Among the pegmatite intrusions, one displays an alkaline syenite composition and includes albite, K-feldspar, quartz, biotite, alkaline amphibole and brannerite (Wülser, 2009). Other brannerite occurrences (not studied) are within quartz-ilmenite veins such as Charlotte and Jacob mineralisations characterised by large euhedral brannerite crystals (Wülser, 2009).

The El Cabril (EC) occurrence is located in the Sierra Albarrana, Andalusia (Spain). This massif belongs to the late Proterozoic to Lower Cambrian Ossa Morena zone and is mainly composed of paragneisses, micaschists and garnet-bearing amphibolites (González del Tánago and Arenas, 1991; Azor and Ballèvre, 1997). Metamorphic rocks are cross cut by pegmatite intrusions, which are composed of quartz, K-feldspar, albite, muscovite, tourmaline, garnet, biotite, monazite, ilmenite, rutile and primary uranium minerals, such as brannerite and uraninite (Garotte *et al.*, 1980; Contreras *et al.*, 1983). Age of brannerite crystallisation is unknown but is not older than the Devonian thermal event (351Ma – 391Ma) recorded by amphibolite and metapelite in the Sierra Albarrana (Dallmeyer and Quesada, 1992).

The Lodrino (BR1) pegmatite in Ticino, Switzerland crosscuts the Variscan orthogneisses of the Leventina Nappe (Rütti *et al.*, 2008) and is mainly composed of quartz and orthoclase, with minor albite, muscovite, brannerite, molybdenite, scheelite, apatite, titanite, powellite and rutile (Bianconi and Simonetti, 1967). Age of pegmatite emplacement is unknown, but it is probably related to the well-known Tertiary pegmatite field that extends over Southwestern Switzerland (Wenk, 1970; Burri *et al.*, 2005). This area overlaps the zone of alpine migmatisation and available U-Pb geochronological constrains span between 29 and 20 Ma (Guastoni *et al.*, 2014). This age is significantly older than the K-Ar age at ca. 11.4 Ma reported for the Lengenbach brannerite mineralization in Eastern Valais (Purdy and Stalder, 1973; Graeser and Guggenheim, 1990).

Sample NA12 is a single crystal from a pegmatite collected along the Marienfluss Valley, to the West of Hartmann Mountains, Northern Namibia. This pegmatite is intrusive within the Paleoproterozoic Epupa Metamorphic Complex, made of migmatised granitoid gneisses with rare intercalations of metasediments (Kröner *et al.*, 2010). This unit was intruded by Mesoproterozoic granitoids related to extension in the Southern Congo craton (Kröner and Rojas-Agramonte, 2017) and further experienced further overprinting due to the late Neoproterozoic to early Palaeozoic Pan-African event related to the Kaoko orogeny (Goscombe *et al.*, 2003). This later event, characterised by polyphase deformation and magmatism has produced biotite-muscovite pegmatite dykes, especially in the Hartmann Mountains (Goscombe *et al.*, 2005); sample (NA12) is spatially related to this ca. 500 Ma episode (Goscombe *et al.*, 2005), but further studies are required to confirm this hypothesis.

Table A1. Standard used for calibration of EPMA data.

Element	Standard formula	Diffraction crystal	Analysed radiation line	Counting time for peak (s)
U	UO_2	PET	*M*α	20
Ti	$MnTiO_3$	LPET	*K*α	20
Si	Albite	TAP	*K*α	10
Al	Al_2O_3	TAP	*K*α	10
Fe	Fe_2O_3	LIF	*K*α	20
Ca	Andradite	PET	*K*α	20
Ba	$BaSO_4$	LIF	*L*α	20
Mn	$MnTiO_3$	LIF	*K*α	20
Mg	Olivine	TAP	*K*α	20
Y	YPO_4	TAP	*L*α	20
Ce	$CePO_4$	LPET	*L*α	20
Nd	$NdPO_4$	LIF	*L*α	20
Pb	PbS	LPET	*M*α	20
Th	ThO_2	PET	*M*α	20

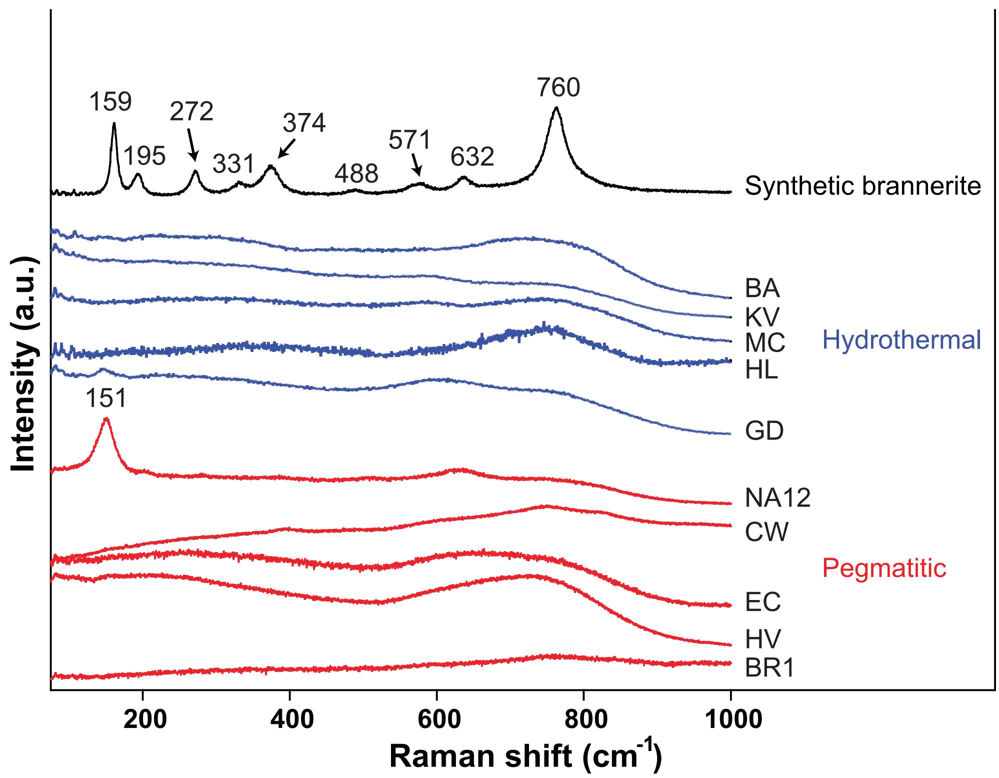

Fig. A1. Raman spectra of a synthetic brannerite and studied natural brannerite samples. The synthetic brannerite sample comes from Mesbah *et al*. (2019). The characteristic vibrational Raman modes of synthetic brannerite are at 760 cm^{-1} (antisymmetric stretching vibration of the (Ti–O–Ti) moiety), 195, and 159 cm^{-1} (lattice external modes, see Zhang *et al*. (2013) and Mesbah *et al*. (2019) for a complete assignment of the Raman vibration modes). Spectra of natural samples were acquired in unaltered domain (Figs 3,6). Abbreviations: BA: Bou Azzer; KV: Kratka Valley; MC: Mont Chemin; HL: Himalaya; GD: La Gardette; NA12: Namibia; CW: Crocker's Well; EC: El Cabril; HV: Hidden Valley; BR1: Lodrino.

References

Ansermet S. (2001) *Le Mont Chemin*. Nouvelles Imprimeries Pillet, Martigny, Suisse, 302 pp.

Ashley P.M. (1984) Sodic granitoids and felsic gneisses associated with uranium-thorium mineralisation, Crockers Well, South Australia. *Mineralium Deposita*, **19**, 7–18.

Azor A. and Ballèvre M. (1997) Low-Pressure Metamorphism in the Sierra Albarrana Area (Variscan Belt Iberian Massif). *Journal of Petrology*, **38**, 35–64.

Barféty J.-C., Bordet P., Carme F., Debelmas J., Meloux M., Montjuvent G., Mouterde R. and Sarrot-Reynauld J. (1972). Carte géologique détaillée de la France à 1/50.000°, feuille Vizille, *BRGM*, Geological Map.

Bianconi F. and Simonetti A. (1967) La brannerite e la sua paragenesis nelle pegmatite di Lodrino (Ct. Ticino). *Schweizerische Mineralogische und Petrographische Mitteilungen*, **47**, 887–934.

Burri T., Berger A. and Engi M. (2005) Tertiary migmatites in the Central Alps: Regional distribution field relations conditions of formation and tectonic implications. *Schweizerische Mineralogische und Petrographische Mitteilungen*, **85**, 215–232.

Campana B. and King D. (1958). Regional geology and mineral resources of the Olary province. *Geological Survey of South Australia Bulletin*, **30**, 7–50.

Coats R.P. and Blissett A.H. (1971) Regional and Economic Geology of the Mount Painter Province. *Geological Survey of South Australia Bulletin*, Vol. 43, Adelaide, 426 pp.

Contreras M.C., Garrote A. and Sánchez-Carretero R. (1983) Pegmatitas en materiales metamórficos del norte de la provincia de Córdoba: mineralogía y posibilidades económicas. *Cuad Lab Xeol Laxe*, **6**, 415–428.

Copeland P., Harrison T.M., Hodges K.V., Maruéjol P., Lefort P. and Pecher A. (1991) An early pliocène thermal disturbance of the main central thrust central Nepal: Implications for Himalayan tectonics. *Journal of Geophysical Research*, **96**, 8475–8500.

Cuney M. (2010) Evolution of uranium fractionation processes through time: driving the secular variation of uranium deposit types. *Economic Geology*, **105**, 553–569.

Dallmeyer R.D., Quesada C. (1992) Cadomian vs. variscan evolution of the Ossa Morena Zone (SW Iberia): field and 40Ar/30Ar mineral age constraints. *Tectonophysics*, **216**, 339–364.

Ennaciri A. (1995) *Contribution a l'étude du district a Co, As, (Ni, Au, Ag) de Bou Azzer Anti Atlas (Maroc), données mineralogiques et geochimiques; étude des inclusions fluids*. PhD dissertation Université d'Orléans France.

Ennaciri A., Barbanson L. and Touray J.-C. (1997) Brine inclusions from the Co-As(Au) Bou Azzer district, Anti-Atlas Mountains, Morocco. *Economic Geology*, **92**, 360–367.

Foden J., Elburg M.A., Dougherty-Page J. and Burtt A. (2006) The timing and duration of the Delamerian Orogeny: correlation with the Ross Orogen and implications for Gondwana Assembly. *Journal of Geology*, **114**, 189–210.

Garotte A., Ortega Huertas M. and Romero J. (1980) Los yacimentos de pegmatitas de Sierra Albarrana (Provincia de Cordoba Sierra Morena). Pp. 145–168 in: *La Reunion sobre la geologia de Ossa-Morena*. Temas Geologica Minros, Madrid.

Gasquet D., Bertrand J.-M., Paquette J.-L., Lehmann J., Ratzov G., Guedes R.A., Tiepolo M., Boullier A.-M., Scaillet S. and Nomade S. (2010) Miocene to Messinian deformation and hydrothermal activity in a pre-Alpine basement massif of the French western Alps: new U–Th–Pb and argon ages from the Lauzière massif. *Bulletin de la Société Géologique de France*, **181**, 227–241.

Geffroy J. (1963) La brannerite du filon aurifere de la Gardette (Isere) et sa signification metallogenique. *Bulletin de la Société de France de Minéralogie et Cristallographie*, **86**, 129–132.

González del Tánago J., Arenas R. (1991) Amfibolitas graatiferas de Sierra Albarrana (Cordoba). Termobarometria e implicaciones para el desarrollo del metamorfismo regional. *Revista de la Sociedad Geologica de Espana* **4** 251–269.

Goscombe B.D., Hand M., Gray D. and Mawby J. (2003) The metamorphic architecture of a transpressional orogen: the Kaoko Belt Namibia. *Journal of Petrology*, **44**, 676–711.

Goscombe B., Gray D., Armstrong R., Foster D.A. and Vogl J. (2005) Event geochronology of the Pan-African Kaoko Belt Namibia. *Precambrian Research*, **140**, 103.e1–103e41.

Graeser S., Guggenheim R. (1990) Brannerite from Lengenbach Binntal (Switzerland). *Schweizerische Mineralogische und Petrographische Mitteilungen*, **70**, 325–331.

Guastoni A., Pennacchioni G., Pozzi G., Fioretti A.M., Walter J.M. (2014) Tertiary pegmatite dikes of the Central Alps. *The Canadian Mineralogist*, **52**, 191–219.

Kissin S.A. (1992) Five-element (Ni–Co–As–Ag–Bi) veins. *Geoscience Canada*, **19**, 113–124.

Kröner A., Rojas-Agramonte Y. (2017) Mesoproterozoic (Grenville-age) granitoids and supracrustal rocks in Kaokoland northwestern Namibia. *Precambrian Research*, **98**, 572–592.

Kröner A., Rojas-Agramonte Y., Hegner E., Hoffmann K.-H. and Wingate M.T.D. (2010) SHRIMP zircon dating and Nd isotope systematics of Palaeoproterozoic migmatitic orthogneisses in the Epupa Metamorphic Complex of NW Namibia. *Precambrian Research*, **183**, 50–69.

Leblanc M. and Billaud P. (1982) Cobalt arsenide ore bodies related to an upper Proterozoic ophiolite; Bou Azzer (Morocco). *Economic Geology*, **77**, 162–175.

Leblanc M. and Lbouabi M. (1988) Native silver mineralization along a rodingite tectonic contact between serpentinite and quartz diorite (Bou Azzer Morocco). *Economic Geology*, **83,** 1379–1391.

Leblanc M. (1986) Co-Ni arsenide deposist with accessory gold in ultramafic rocks from Morocco. *Canadian Journal of Earth Science*, **23**, 1592–1602.

Ludwig K.R. and Cooper J.A. (1984) Geochronology of Precambrian granites and associated U–Ti–Th mineralization northern Olary province South Australia. *Contributions to Mineralogy and Petrology*, **86**, 298–308.

Marshall D., Meisser N. and Taylor R.P. (1998) Fluid inclusion stable isotope and Ar-Ar evidence for the age and origin of gold-bearing quartz veins at Mont Chemin Switzerland. *Mineralogy and Petrology*, **62**, 147–165.

Maruejol P. (1988) *Métasomatose alcaline et mindralisations uranifères: les albitites du gisement de Lagoa Real (Bahia Brésil) et exemples complémentaires de Xihuashan (SE Chine) Zheltorechensk (Ukraine) et Chhuling Khola (Népal central).* PhD dissertation, Insitut National Polytechnique de Lorraine, Nancy, France.

Meisser N. (1998) La géologie et les concentrations minérales du Mont Chemin. *Minaria Helvetica*, **18b**, 66–82.

Mesbah A., Szenknect S., Clavier N., Lin H., Baron F., Beaufort D., Batonneau Y., Mercadier J., Eglinger A., Turuani M., Goncalves P., Choulet F., Chapon V., Seydoux-Guillaume A.-M., Pagel M. and Dacheux N. (2019) Direct synthesis of pure brannerite UTi_2O_6. *Journal of Nuclear Materials*, **515**, 401–406.

Oberthür T., Melcher F., Henjes-Kunst F., Gerdes A., Stein H., Zimmerman A. and El Ghorfi M. (2009) Hercynian age of the cobalt-nickel-arsenide-(gold) ores Bou Azzer Anti Atlas Morocco: Re–Os Sm–Nd and U–Pb age determinations. *Economic Geology*, **104,** 1065–1079.

Purdy J.W. and Stalder H.A. (1973) K-Ar Ages of Fissure Minerals from the Swiss Alps. *Schweizerische Mineralogische und Petrographische Mitteilungen*, **53**, 79–98.

Rojkovic I. and Boronikhin V.A. (1982) U-Ti minerals at the deposit Novoveska Huta (Slovenske Rudohorie Mts.). *Geologicky Zbornik*, **33**, 321–330.

Rojkovic I., Novotny L. and Haber M. (1993) Stratiform and vein U Mo and Cu mineralization in the Novoveskfi Huta area CSFR. *Mineralium Deposita*, **28**, 58–65.

Rütti R., Marquer D. and Thompson A.B. (2008) Tertiary tectono-metamorphic evolution of the European margin during Alpine collison: example of the Leventina Nappe (Central Alps Switzerland). *Swiss Journal of Geosciences*, **101**, S157–S171.

Števko M., Uher P., Ondrejka M., Ozdín D and Bačík P. (2014) Quartz–apatite–*REE* phosphates–uraninite vein mineralization near Čučma (eastern Slovakia): a product of early Alpine hydrothermal activity in the Gemeric Superunit Western Carpathians. *Journal of Geosciences*, **59,** 209–222.

Vozárová A., Šarinová K., Sergeev S., Larionov A. and Presnyakov S. (2010) Late Cambrian/Ordovician magmatic arc type volcanism in the Southern Gemericum basement Western Carpathians Slovakia: U–Pb (SHRIMP) data from zircons., *International Journal of Earth Sciences*, **99**, 17–37.

Vozárová A., Konecný P., Šarinová K. and Vozár J. (2014) Ordovician and Cretaceous tectonothermal history of the Southern Gemericum Unit from microprobe monazite geochronology (Western Carpathians Slovakia)., *International Journal of Earth Sciences*, **103**, 1005–1022.

Wenk E. (1970) Zur Regionalmetamorphose und Ultrametamorphose im Lepontin. *Fortschritte der Mineralogie*, **47**, 34–51.

Wülser P.-A. (2009) *Uranium metallogeny in the North Flinders Ranges region of South Australia*. PhD dissertation, Adelaide University, Australia.

Zhang Y.J., Karatchevtseva I., Qin M.J., Middleburgh S.C. and Lumpkin G.R. (2013) Raman spectroscopic study of natural and synthetic brannerite *Journal of Nuclear Materials*, **437**, 149–153.